

New Crystal-Assisted Pair-Creation Process

J. C. Kimball, N. Cue, L. M. Roth, and B. B. Marsh

Department of Physics, State University of New York at Albany, Albany, New York 12222

(Received 24 January 1983)

The electron-positron pair production for a beam of very energetic photons (or ultra-relativistic charged particles) is predicted to be significantly enhanced when the beam is aligned along crystallographic rows of atoms. Channeling in crystals lowers the total energy of the created electron thus enabling the photon to decay in a one-step process. The new mechanism yields a rapidly increasing flux of electrons and positrons of comparable energies above a threshold near 30 GeV.

PACS numbers: 12.20.Ds, 61.80.Mk, 79.20.Kz

A new electron-positron pair production process is predicted to occur when very energetic photons (or charged particles) are directed along crystallographic axes or planes. This pair production is special because it is related to a solid-state effect. The crystal field in the solid lowers the energy of some electrons by the well-established "channeling" effect,¹ so that a photon can decay directly into an electron-positron pair while conserving both energy and momentum. The physics of this pair production is in some ways analogous to "strong-field" electron-positron production. It has long been known that the Dirac equation "breaks down" for systems with very large fields. For example, there is no ground-state solution for hydrogenic atoms with nuclear point charges larger than 137. If very heavy nuclei could be produced, even for a short instant of time, one would expect the spontaneous generation of electron-positron pairs.² Similarly, in the coordinate system of an energetic charged particle moving along a row of atoms, the effective field is very large because of the Lorentz contraction of the atomic spacing along the row. In this reference frame, matrix elements and energy criteria used to calculate pair production by an energetic photon in a crystal are formally similar to a calculation of the spontaneous generation of electron-positron pairs which would be produced by a very deep two-dimensional potential well.

The enhanced pair production is best illustrated by first considering the channeling states of energetic electrons produced by a perfectly aligned photon beam. For concreteness, we work in a crystal-based coordinate system and discuss only the axial case in which a single-string approximation is adequate for the tightly bound states. Averaging effects of the particle's rapid motion along the string of atoms (taken to lie along the z axis) results in a crystal potential $V(\rho)$ which

depends only on the transverse coordinate $\rho = (x^2 + y^2)^{1/2}$. With this potential, momentum along the z axis is conserved and the spatial wave function of the electron with longitudinal momentum p is (in units where $\hbar = c = 1$)

$$\psi(\vec{r}) = e^{ipz} \varphi^-(\vec{\rho}). \quad (1)$$

The total energy of the electron, $E^- = \gamma^- m$, is the sum of a free-particle energy for motion along z , and a transverse energy ϵ^- for motion in the $\vec{\rho}$ plane:

$$E^- = (m^2 + p^2)^{1/2} + \epsilon^-. \quad (2)$$

In the relativistic limit, the Dirac equation reduces to the following two-dimensional Schroedinger equation which describes the transverse motion³:

$$\left[\frac{-1}{2\gamma^- m} \left(\frac{\partial^2}{\partial x^2} + \frac{\partial^2}{\partial y^2} \right) - eV(\rho) \right] \varphi^-(\vec{\rho}) = \epsilon^- \varphi^-(\vec{\rho}). \quad (3)$$

Since an electron can be bound by the potential $-eV(\rho)$, the spectrum of transverse energy levels for the electron includes a discrete set of negative-energy levels (denoted by ϵ_j^-), as well as a positive continuum. Indeed, observations of channeling radiation over a wide beam-energy range are manifestations of such bound states.⁴ With very energetic electrons, the large relativistic mass gives rise to a ground-state binding energy $|\epsilon_0^-|$ which is nearly the same as the depth of the potential well.

An analogous Schroedinger equation applies to the positron wave function $\varphi^+(\rho)$, where the positron relativistic factor γ^+ replaces γ^- , and the sign of the electric charge is changed. However, the physical properties of the positron states are different because they are never bound by the electrostatically positive string potential. For convenience, we enclose the system in a box so that for each quantized positron momentum, the transverse positron states can be indexed by an

integer k . Both electron and positron states are shown in Fig. 1 in the form of an energy-momentum dispersion relation for particles moving along the z axis in the crystal. The uppermost and lowermost curves correspond to unbound positive- and negative-energy solutions to the Dirac equation. The dispersion relation for an electron in one of the bound states of the two-dimensional string potential is also shown. For purposes of illustration, the depth of the potential is exaggerated so that the downward displacement of the bound electron's energy can be displayed. In real crystals, the much shallower potential leads to a much smaller binding energy.

The binding of the high-momentum electron states in a two-dimensional potential allows the new process of pair production to take place. This is illustrated in Fig. 1 by the wavy line representing the photon excitation of an electron from an occupied negative-energy state to one of the bound positive-energy states. By directly absorbing a photon's energy and momentum, a

particle makes a transition in a direction parallel to the photon dispersion curve labeled as the photon line. A Feynman diagram illustrating the production of the electron with momentum p , and the positron with momentum $q - p$, by a photon with momentum q (along z) is illustrated in the inset to Fig. 1. The electron final state is shown as a double line to emphasize its bound-state character. This new process should be contrasted to the ordinary mechanism of pair production⁵ where nuclear scattering is required to conserve energy, and coherent pair production⁶ in which the scattering momentum is a reciprocal-lattice vector.

A very large threshold energy for the direct production of electron-positron pairs can also be seen in Fig. 1. For ultrarelativistic velocities, E^- and E^+ can be expanded to lowest order in m . Then conservation of energy and longitudinal momentum yields a condition on the transverse energies of the created pair,

$$\epsilon_k^+ = |\epsilon_j^-| - \frac{1}{2}m(1/\gamma^- + 1/\gamma^+). \quad (4)$$

Since ϵ_k^+ must be positive (no positron binding), $1/\gamma^- + 1/\gamma^+$ must be less than $2|\epsilon_0^-|/m$ before any transition can take place. At the kinematic threshold for direct pair creation, γ^+ and γ^- will be equal, and the photon threshold energy is

$$q_{th} = 2m^2/|\epsilon_0^-|. \quad (5)$$

Typical values for electron binding energies $|\epsilon_0^-|$ yield threshold energies of several gigaelectronvolts.

In our computation of the pair production rate, the transition matrix element for the process displayed in Fig. 1 is calculated by adding the photon field to the Dirac equation. This quantity, involving four-component spinors and Dirac matrices, can be transformed into matrix elements of the Schrodinger-like electron and positron wave functions. The transformation yields spin and orbital matrix elements which are of comparable magnitude. A spin matrix element produces an electron and positron with spins polarized along the direction of the photon spin. Two orbital matrix elements convert the angular momentum of the photon into a net orbital angular momentum of the electron-positron pair. Since all particles are plane-wave-like in the z direction, these matrix elements reduce to overlap integrals of electron and positron wave functions in the ρ plane. With the photon polarized along the $+z$ axis, the spin matrix element for the

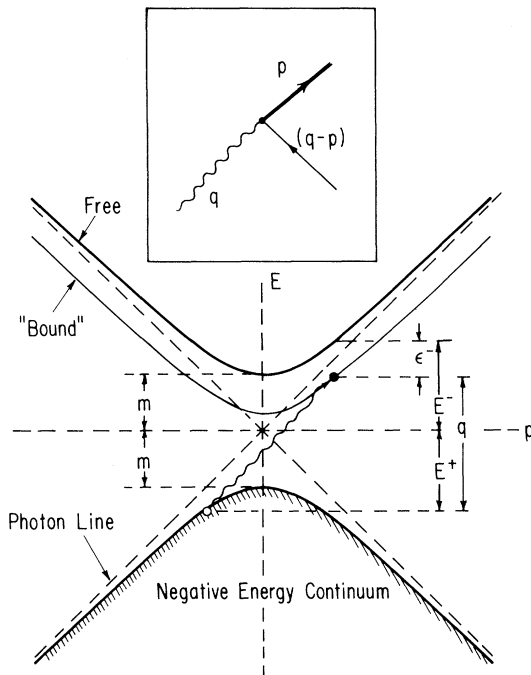


FIG. 1. A new crystal-assisted process of electron-positron pair production, shown for an incident high-energy photon aligned along a crystal axis. Both energy and longitudinal momentum are conserved in the one-step process of exciting an electron from the negative-energy continuum to a positive-energy channeling bound state. The binding energy has been exaggerated for purposes of illustration. The inset is the corresponding Feynman diagram.

creation of a spin-up electron in the j th bound state with momentum p , and a spin-up positron in the k th continuum state with momentum $q - p$, is

$$M(p, k)_{j1} = e(\pi/q\Omega)^{1/2}(1/\gamma^- + 1/\gamma^+) \times \int \varphi_j^-(\vec{p})^* \varphi_k^+(\vec{p}) d^2\rho. \quad (6)$$

One of the corresponding orbital matrix elements is

$$M(p, k)_{j2} = e(\pi/q\Omega)^{1/2}(E^+)^{-1} \times \int \varphi_j^-(\vec{p})^* (p_x + ip_y) \varphi_k^+(\vec{p}) d^2\rho \quad (7)$$

for a spin-up electron and spin-down positron. The other orbital term $[M(p, k)_{j3}]$ is obtained by replacing E^+ by E^- and reversing the spins of both the electron and positron. For all of the matrix elements, q is the photon energy, Ω is the volume of crystal associated with one string of atoms, and p_x and p_y are momentum operators in the x and y direction. The integrals determining these matrix elements are small because the electron-positron overlap is small.

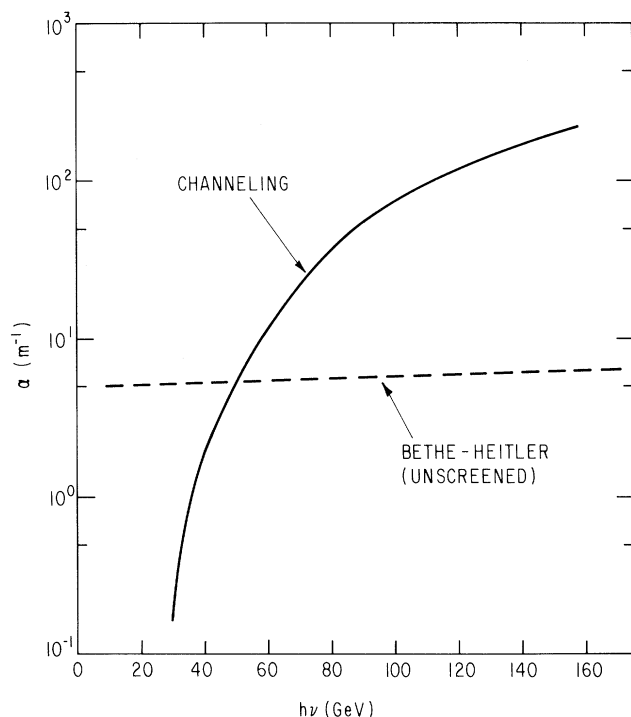


FIG. 2. Numerical predictions of the absorption coefficient (inverse mean free path), α , for the process described in Fig. 1 as a function of the incident photon energy for the case of perfect alignment along the $\langle 110 \rangle$ axis of diamond. The corresponding Bethe-Heitler results for incoherent binary collisions (random alignment) are shown for comparison.

The potential which binds the electron repels the positron, and the overlap is nonzero only because of barrier penetration. With use of the Golden Rule, the transition rate W is then

$$W = 2\pi \sum_{p, k, j, i} |M(p, k)_{ji}|^2 \times \delta(\epsilon_k^+ + \epsilon_j^- + \frac{1}{2}m(1/\gamma^- + 1/\gamma^+)), \quad (8)$$

with the delta function assuring conservation of energy as described in Eq. (4). The important aspect of the calculation is that only the photon field is taken as the perturbation. The crystal field is included in the zero-order Hamiltonian so that the final states correspond to an electron and positron in the crystal, not in vacuum.⁷

Numerical results of our calculations are shown in Figs. 2 and 3 for the specific case of incident photons aligned along the $\langle 110 \rangle$ axis of diamond. For the transverse potential, the Lindhard standard type has been used in which the effect of thermal displacements of lattice atoms is simulated by the substitution $\rho^2 \rightarrow \rho^2 + u^2/2$, where u is the mean thermal displacement amplitude in two dimensions. Matrix elements $M(p, k)_{ji}$ were calculated with use of the WKB approximation for both bound electron and continuum positron states. The results were checked with variational wave functions. A reasonable agreement was obtained with results of a simpler calculation which linearized the potential in the neighborhood of the classical turning points. Figure 2 dis-

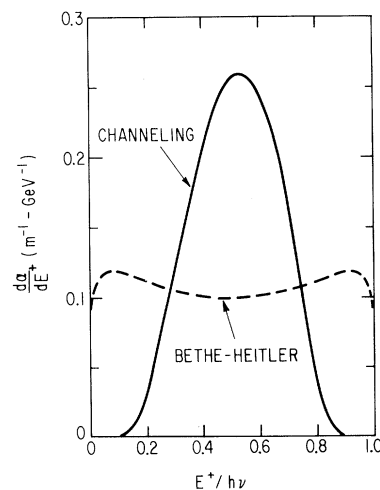


FIG. 3. The predicted positron energy distribution for the process described in Fig. 1 for 51.1-GeV photons directed along the $\langle 110 \rangle$ direction in diamond. The corresponding Bethe-Heitler result for a random direction is shown for comparison.

plays the absorption coefficient (inverse of the mean free path) $\alpha = W/c$ as a function of the incident photon energy. The crystal-assisted rate is very small for low energies, but it increases rapidly with energy, and exceeds the Bethe-Heitler results at high energy. An increasing wave-function overlap in the matrix elements is primarily responsible for the growth in the absorption coefficient. In this example, the kinematic threshold is only 3 GeV, and the apparent threshold near 30 GeV is a matrix-element effect.

The differential rate of pair production is obtained similarly except that no summation over positron momenta is performed. The result is shown in Fig. 3 for a photon energy of 51.1 GeV. A characteristic feature is evident; unlike in the Bethe-Heitler result, most positrons receive about $\frac{1}{2}$ the photon energy. This is again a reflection of the matrix elements. The positron barrier penetration increases with ϵ_k^+ and, according to Eq. (4), ϵ_k^+ is largest when $\gamma^- = \gamma^+$.

The theory and predictions described so far are confined to the rather restrictive case of a perfectly aligned incident photon. Misalignment by an angle $\theta = q_\perp/q$ introduces a photon phase factor $\exp(-i\vec{q}_\perp \cdot \vec{p})$ in the integrand of Eqs. (6) and (7). The additional energy supplied by the transverse photon momentum changes the energy relation in Eq. (4). Approximate calculations for this case show that there is a small critical angle beyond which the crystal-assisted pair production falls off quickly.

We also predict similar enhancement effects for any incident charged particle, since it can produce both real and virtual photons, and both types can lead to pair creation. For an incident electron or positron, the threshold energy is roughly twice that for incident photons. There

is, however, one important distinction between electrons and positrons. The positrons will be repelled from the atomic rows and thus their pair production rate should be smaller than that for incident electrons. Enhanced pair production should also be manifested for particles incident in planar directions, but because the transverse potential is weaker, the corresponding threshold energy is higher. Finally, there may be important implications if this new process is confirmed. The relatively large pair production rate and narrow pair energy distribution function expected for incident ultrarelativistic electrons can give rise to a relatively intense and monoenergetic positron beam.

We gratefully acknowledge important conversations with Professor Akira Inomata. One of us (J. K.) was supported by a Cottrell Research Corporation grant.

¹See, e.g., D. S. Gemmell, *Rev. Mod. Phys.* **46**, 129 (1974).

²See, e.g., J. Reinhardt, B. Muller, and W. Greiner, *Phys. Rev. A* **24**, 103 (1981).

³V. V. Beloshitskii and M. A. Kumahkov, *Zh. Eksp. Teor. Fiz.* **74**, 1244 (1978) [*Sov. Phys. JETP* **4**, 652 (1978)].

⁴See, e.g., in *Proceedings of the Ninth International Conference on Atomic Collisions in Solids, Lyon, France, 1981*, edited by J. Remillieux, J. C. Poizat, and M. J. Gaillard (North-Holland, Amsterdam, 1982), pp. 209–253.

⁵W. Heitler, *The Quantum Theory of Radiation, Third Edition* (Oxford Univ. Press, London, 1960), pp. 256–267.

⁶G. D. Palazzi, *Rev. Mod. Phys.* **40**, 611 (1968).

⁷This differs from earlier descriptions of crystal effects on pair production; see, e.g., F. J. Dyson and H. Überall, *Phys. Rev.* **99**, 604 (1955), and Ref. 6.